EPJ Web of Conferences **172**, 02002 (2018) https://doi.org/10.1051/epjconf/201817202002
ISMD 2017

Cross-section measurements of final states with photons and jets with the ATLAS experiment

Miguel Villaplana Pérez[1,⋆], on behalf of the ATLAS Collaboration

[1] *INFN Milano*

Abstract.
The ATLAS Collaboration has performed precise measurements of the cross-section of final states with photons and/or jets at centre-of-mass energies of 8 and 13 TeV. The results are compared with state-of-the-art theory predictions and with predictions of several Monte Carlo generators. We also present new measurements of transverse energy-energy correlations and their associated asymmetries in multi-jet events at 8 TeV. Both measurements are used to extract the strong coupling constant and test the renormalization group equations.

1 Introduction

ATL-PHYS-PROC-2017-231
15/12/2017

The modeling of a proton-proton collision at the Large Hadron Collider (LHC) can be divided in four main steps. The hard-scatter process is described by perturbative quantum chromodynamics (pQCD) and it depends on the parton distribution function (PDF) of the protons. The partons resulting from the hard-scatter process are taken to the non-perturvatibe regime through parton emission and splitting in the fragmentation process. Hadronisation evolves the confined quarks to the state we observe in the ATLAS detector [1]. Color-connected beam–beam remnants and multiple-parton interactions within the colliding protons, the "underlying event", are also described by non-perturbative models. Photons are a hard colourless probe of the hard-scatter process, which provides a good test of pQCD calculations and helps constrain the proton PDF. The analyses described in this paper include both photons coming from the matrix element (direct production) and from the fragmentation process. An isolation requirement is applied in order to reduce the background resulting from photons produced during hadronisation.

In the ATLAS experiment, detector-level jets are formed by clustering topological energy clusters from both the hadronic and electromagnetic calorimeters. On the simulations side, the particles resulting from the fragmentation and the hadronisation are clustered into particle-level jets. When only parton-level predictions are available, these are first clustered into jets, which are then corrected to account for the effect of fragmentation and hadronisation. Monte Carlo (MC) simulations are used to correct the effects of detector efficiency and resolution in both photon and jet measurements in order to compare them to theory predictions at particle level. This allows ATLAS data not only to be confronted to PDF models and perturbative calculations but also to test the modeling of factorisation and hadronisation.

⋆e-mail: Miguel.Villaplana.Perez@cern.ch

The production of jets and prompt isolated photons at hadron colliders provides a stringent test of pQCD and can be used to probe the proton structure. The production of prompt photons in association with jets provides an additional testing ground for pQCD with a hard colourless probe less affected by hadronisation effects than jet production. Jet production can also be used to probe the gluon density function of the proton. Specific topologies can be used to extract the strong coupling constant.

This paper presents recent measurements of the cross-section of final states involving photons or jets at center-of-mass energies of 8 and 13 TeV performed by the ATLAS Collaboration. We also present new measurements of transverse energy-energy correlations (TEEC) and their associated asymmetries (ATEEC) in multi-jet events at 8 TeV and the extraction of the strong coupling constant from them.

2 Photon production

2.1 Inclusive isolated photon production

Inclusive isolated photon production at 13 TeV has been studied using a data set with an integrated luminosity of 3.2 fb^{-1} [2]. Cross-sections as a function of E_T^γ are measured in four different regions of η^γ for photons with $E_T^\gamma > 125$ GeV and $|\eta^\gamma| < 2.37$. Values of E_T^γ up to 1.5 TeV are measured. The predictions of the Pythia [3] and Sherpa [4] Monte Carlo models give a good description of the shape of the measured cross-section distributions except for $E_T^\gamma \gtrsim 500$ GeV in the regions $|\eta^\gamma| < 0.6$ and $0.6 < |\eta^\gamma| < 1.37$.

Figure 1 shows the individual components of the systematic uncertainties added in quadrature in representative phase-space regions. Photon energy scale is the dominant uncertainty at high E_T^γ, while at low E_T^γ it is the uncertainty related to the background subtraction method that dominates. Uncertainties are larger in the forward regions.

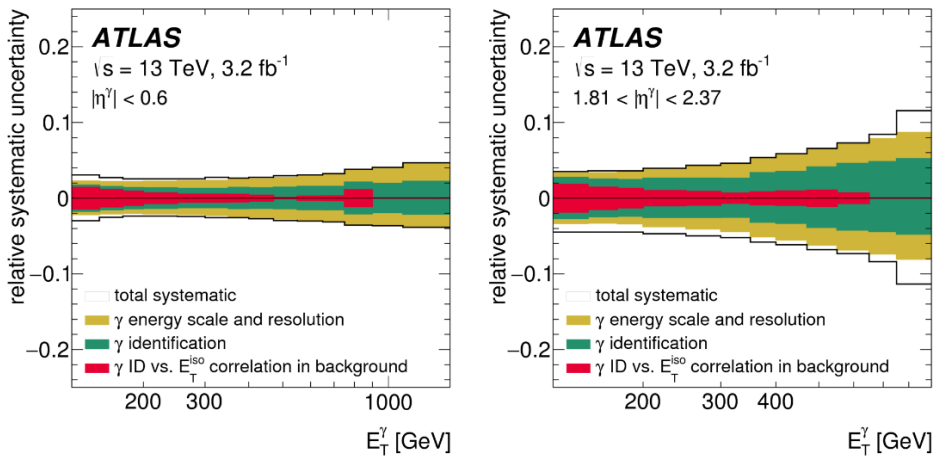

Figure 1. Total relative systematic uncertainty, excluding that in the luminosity measurement, as a function of E_T^γ (black histogram) as well as the contributions from the photon energy scale and resolution (yellow histogram), the photon identification (green histogram) and the photon identification vs. E_T^{iso} correlation in the background (red histogram) in $|\eta^\gamma| < 0.6$ (right) and $1.81 < |\eta^\gamma| < 2.37$ (left). The histograms show the stacked contributions [2].

The NLO pQCD predictions, using Jetphox [5] and based on different sets of proton PDFs, provide an adequate description of the data within the experimental and theoretical uncertainties. For most of the phase space the theoretical uncertainties are larger than those of experimental nature and dominated by the terms beyond NLO, from which it is concluded that NNLO pQCD corrections are needed to make an even more stringent test of the theory. The ratios of the theoretical predictions based on different PDF sets to the measured cross-sections are found to be very similar, the differences being much smaller than the theoretical scale uncertainties.

NNLO predictions have been also compared to ATLAS inclusive photon measurements at 8 TeV [7]. These new calculations, displayed in figure 2, show a trend to be above the data at high E_T. Accounting for both NNLO QCD and electroweak effects provides an improved prediction. The theoretical uncertainty is reduced by a factor close to 3 with respect to NLO predictions.

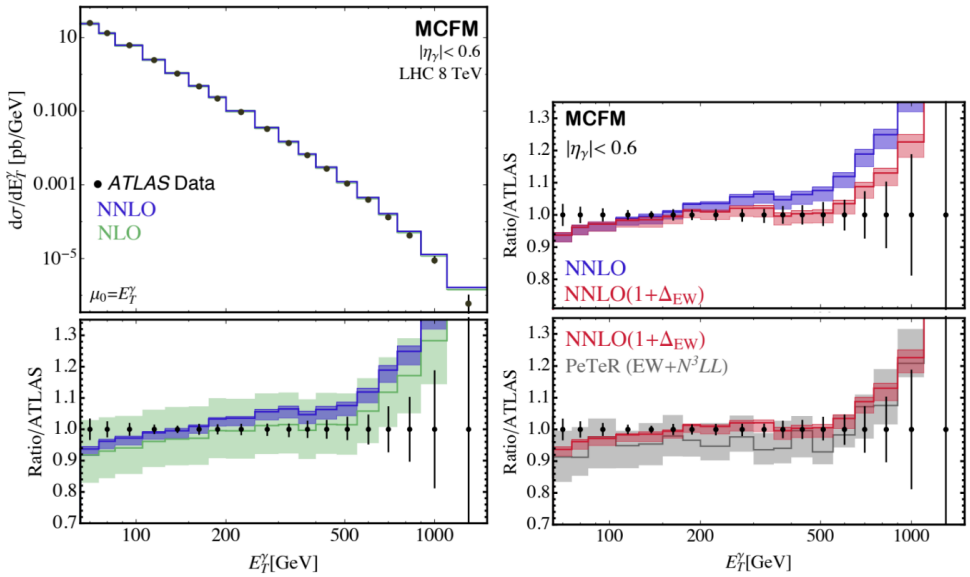

Figure 2. (Left) A comparison of the MCFM predictions [7] for the transverse momentum of the photon to ATLAS 8 TeV data. (Right) Upper: the effect of including electroweak corrections in addition to the NNLO predictions provided by MCFM. Lower: a comparison of the NNLO+EW prediction of MCFM with the N3LL+EW prediction of PeTeR [8].

2.2 Photon pair production

Measurements of the production cross-section of two isolated photons at a center-of-mass energy of 8 TeV have been published [9]. The uncertainties are dominated by systematic effects that have been reduced, compared to the previous ATLAS measurement at 7 TeV, due to an improved method to estimate the background and improved corrections to the modeling of the calorimeter isolation variable in simulated samples.

Predicted cross-sections from fixed-order QCD calculations implemented in DIPHOX [10] and RESBOS [11] at NLO, and in 2γNNLO [12] at NNLO, shown in figure 3, are lower than the data. The relative errors associated to the predictions from DIPHOX (2γNNLO) are 10%–15% (5%–10%).

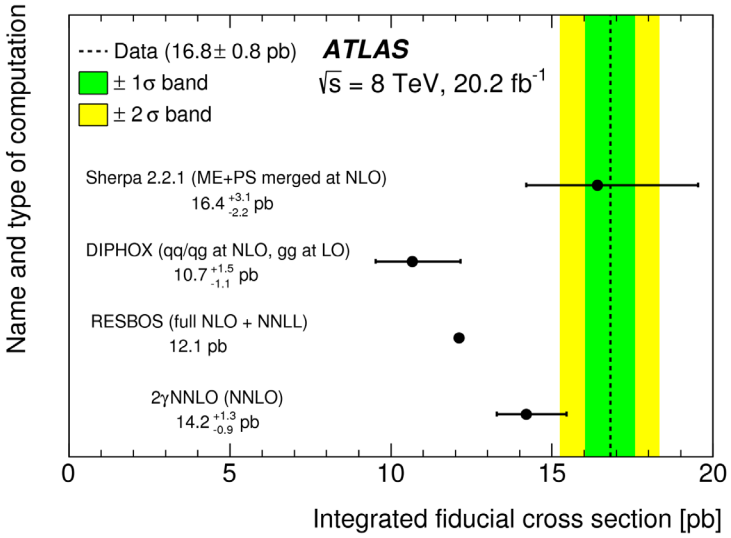

Figure 3. Measured fiducial cross-section compared to the predictions from Sherpa 2.2.1, Diphox, Resbos and 2γNNLO. The uncertainties in the theoretical predictions are shown as horizontal bars. Only the central value is shown for Resbos. The green (yellow) band represents the one- (two-)standard deviation uncertainty, including both the statistical and systematic uncertainties in the measurement added in quadrature [9].

Differential cross-sections are measured as functions of six observables: the diphoton invariant mass, the absolute value of the cosine of the scattering angle with respect to the direction of the proton beams, the opening angle between the photons in the azimuthal plane, the diphoton transverse momentum and two related variables (a_T and ϕ^η), with uncertainties typically below 5% per bin, reaching as high as 25% in a few bins with low numbers of data events.

The effects of infrared emissions, probed precisely by measuring the cross-section as functions of a_T (see figure 4) and ϕ^η, are well reproduced by the inclusion of soft-gluon resummation at the NNLL accuracy. However, in most parts of the phase space, the predictions above are unable to reproduce the data. The discrepancies can reach a factor of 2 in many regions, beyond the theoretical uncertainties, which are typically below 20%.

The predictions of a parton-level calculation of varying jet multiplicity up to NLO matched to a parton-shower algorithm in SHERPA 2.2.1 provide an improved description of the data compared to all the other computations considered in the study and are in good agreement with the measurements, for both the integrated and differential cross-sections.

2.3 Photon plus jet production

Measurements of the cross-sections for the production of an isolated photon in association with one, two or three jets have been studied with the ATLAS detector at 8 TeV [16]. The photon is required to have $E_T^\gamma > 130$ GeV and $|\eta^\gamma| < 2.37$. The jets are reconstructed using the anti-kt algorithm with radius parameter R = 0.6.

The cross-sections for photon plus one jet are measured as functions of E_T^γ and p_T^{jet1} with $p_T^{jet1} > 100$ GeV; the measurements extend up to values of $E_T^\gamma(p_T^{jet1})$ of 1.1 TeV (1.2 TeV). The

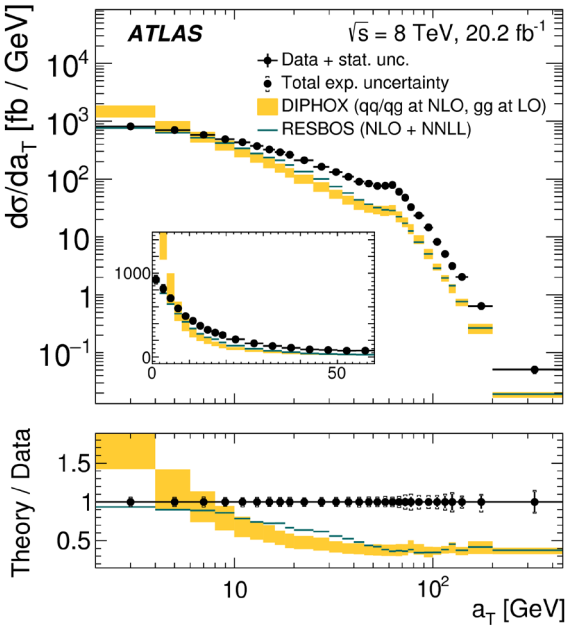

Figure 4. Differential cross-sections as a function of a_T compared to the predictions from Diphox and Resbos. At the bottom, the ratio of the prediction to the data is shown. The bars and bands around the data and theoretical predictions represent the statistical and systematic uncertainties. Only the central values are shown for Resbos. Negative cross-section values are obtained with Diphox in the first bin of a_T and therefore are not shown [9].

dependence on $m_{\gamma-jet1}$ and $|cos\,\theta^*|$ is also measured for $m_{\gamma-jet1} > 467$ GeV and extends up to $m_{\gamma-jet1}$ of 2.45 TeV. The NLO QCD predictions from Jetphox, corrected for hadronisation and underlying-event effects, give a good description of the measured cross-section distributions in both shape and normalisation. In particular, the measured dependence on $|cos\,\theta^*|$ and its scale dependence is consistent with the dominance of processes in which a quark is being exchanged; the experimental (theoretical) uncertainty in $d\sigma/d|cos\theta^*|$ amounts to $\approx 3\%$ (10%).

Photon plus two-jet production is investigated by measuring cross-sections as functions of E_T^{γ}, p_T^{jet2} and angular correlations between the final-state objects for $p_T^{jet1} > 100$ GeV and $p_T^{jet2} > 65$ GeV. The NLO QCD predictions from Blackhat [17] provide a good description of the measurements except for $E_T^{\gamma} > 750$ GeV, as shown on the left panel of figure 5. The predictions from Sherpa, which include higher-order tree-level matrix elements, are found to be superior to those from Pythia, based on $2 \rightarrow 2$ processes, in describing the distributions in p_T^{jet2} and the angular correlations. The patterns of QCD radiation around the photon and the leading jet are compared by measuring the production of the subleading jet in an annular region centred on the given final-state object, β_{object}. The cross-sections as functions of β_{γ} and β_{jet1} are observed to be different. The ratio of the cross-sections (see figure 5) shows enhancements in the directions towards the beams ($\beta = 0$ and π).

Photon plus three-jet production is characterised by measurements of cross-sections as functions of p_T^{jet3} and angular correlations for $p_T^{jet1} > 100$ GeV, $p_T^{jet2} > 65$ GeV and $p_T^{jet3} > 50$ GeV. The NLO QCD predictions from Blackhat provide an adequate description of the measurements. Whereas the prediction from Sherpa for p_T^{jet3} is superior to that from Pythia, both give adequate descriptions of the angular correlations.

The dynamics of isolated-photon production in association with a jet have also been studied using 3.2 fb^{-1} of ATLAS data at 13 TeV [18]. Photons are required to have transverse energies above 125 GeV. Jets are identified using the anti-kt algorithm with radius parameter R=0.4 and required to have transverse momenta above 100 GeV. Measurements of isolated-photon plus jet cross-sections are

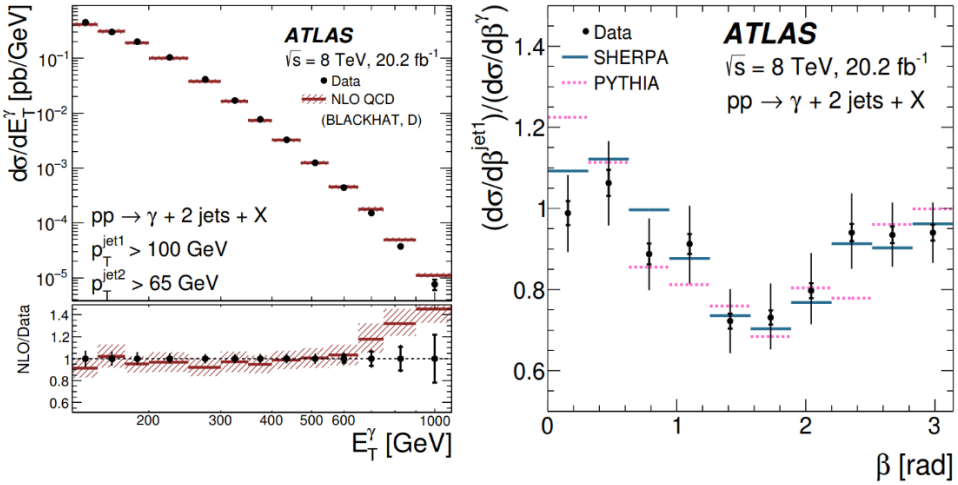

Figure 5. (Left) Measured cross-section for isolated-photon plus two-jet production (dots) as functions of E_T^γ. The NLO QCD predictions from Blackhat corrected for hadronisation and underlying-event effects and using the CT10 PDF set (solid lines) are also shown. These predictions include only the direct contribution (D). The bottom part shows the ratio of the NLO QCD prediction to the measured cross-section. (Right) Ratio of the measured cross-section $d\sigma/d\beta^{jet1}$ and $d\sigma/d\beta^{\gamma}$ (dots); the ratios for the Sherpa and Pythia predictions are shown as solid and dashed lines, respectively. In both figures, the inner (outer) error bars represent the statistical uncertainties (the statistical and systematic uncertainties added in quadrature) and the shaded band represents the theoretical uncertainty. For most of the points, the inner error bars are smaller than the marker size and, thus, not visible [16].

presented as functions of the leading photon transverse energy, the leading jet transverse momentum, the angular separation in azimuth between the photon and the jet, the photon-jet invariant mass and the scattering angle in the photon-jet centre-of-mass system. The measurements extend up to values of 1.5 TeV in E_T^γ and p_T^{jet}, and the dependence on $m_{\gamma-jet}$ and $|cos\ \theta^*|$ is measured for $m_{\gamma-jet} > 450$ GeV.

The predictions of the tree-level plus parton-shower Monte Carlo models Pythia and LO Sherpa give a reasonable description of the shape of the data, except for p_T^{jet} in the case of Pythia. The fixed-order NLO QCD calculations of Jetphox, corrected for hadronisation and underlying-event effects, and the multi-leg NLO QCD plus parton-shower calculations of Sherpa describe the measured cross-sections within the experimental and theoretical uncertainties. The comparison of predictions based on different parameterisations of the proton PDFs shows that the description of the data achieved does not depend significantly on the specific PDF set used. The only meaningful prediction for $d\sigma/d\Delta\phi^{\gamma-jet}$ is that of NLO Sherpa, which is able to reproduce the data down to $\Delta\phi^{\gamma-jet} = \pi/2$ due to the inclusion of the matrix elements for $2 \rightarrow n$ processes with n = 4 and 5. The measured dependence on $|cos\ \theta^*|$, shown in figure 6, is consistent with the dominance of processes in which a quark is being exchanged; the experimental (theoretical) uncertainty on $d\sigma/d|cos\ \theta^*|$ amounts to 3-4% (10% for Jetphox and 15-25% for NLO Sherpa).

All these studies provide stringent tests of pQCD and validate the description of the dynamics of isolated photon in association with jets production in pp collisions at 8 and 13 TeV.

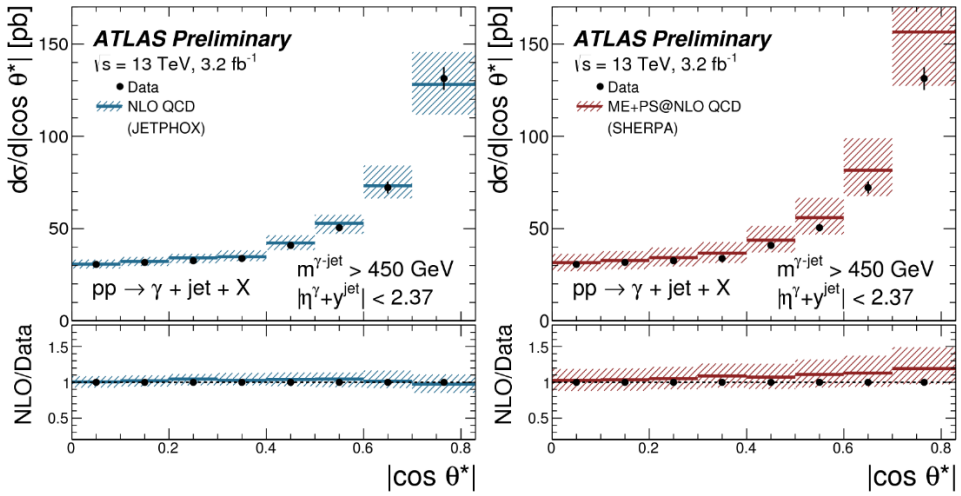

Figure 6. Measured cross-section for isolated-photon plus one-jet production (dots) as a function of $|cos\ \theta^*|$. For comparison, the NLO QCD predictions from JETPHOX corrected for hadronisation and underlying-event effects (left) and the multi-leg NLO QCD plus parton shower predictions from SHERPA (right) are shown with solid lines. The bottom part of each figure shows the ratios of the predictions to the measured cross-section. The inner (outer) error bars represent the statistical uncertainties (the statistical and systematic uncertainties added in quadrature) and the hatched band displays the theoretical uncertainty. For most of the points, the inner error bars are smaller than the marker size and, thus, not visible [18].

3 Jet production

The double-differential inclusive jet cross-sections have been measured using the ATLAS 8 TeV data set. Jets are reconstructed with the anti-kt algorithm with jet radius parameter values of R = 0.4 and R = 0.6, in the kinematic region of the jet transverse momentum from p_T = 70 GeV to about 2.5 TeV and jet rapidities |y| < 3 [13]. The cross-sections are measured double-differentially in the jet transverse momentum and rapidity. The dominant systematic uncertainty arises from the jet energy calibration. Compared to previous jet cross-section measurements a significant reduction of the uncertainties is achieved.

A quantitative comparison of the measurements to fixed-order NLO QCD calculations, corrected for non-perturbative and electroweak effects, shows overall fair agreement (with p-values in the percent range) when considering jet cross-sections in individual jet rapidity bins treated independently. Some tension between data and theory is observed in the central rapidity region for anti-kt jets with R = 0.6. Strong tension between data and theory is observed when considering data points from all jet transverse momentum and rapidity regions, with a full treatment of the correlations. This tension can be reduced, but not completely resolved, using alternative correlation scenarios for the experimental and theoretical two-point systematic uncertainties. The remaining tension could be due either to the breakdown of the assumptions that need to be made in the treatment of two-point systematic uncertainty components, or to an incomplete theoretical description, such as missing higher-order corrections.

The inclusive jet and dijet cross-sections have also been measured using 3.2 fb^{-1} of ATLAS data at 13 TeV [14]. Jets are identified with the anti-kt algorithm with a jet radius parameter value of

R = 0.4. The inclusive jet cross-sections are measured double-differentially as a function of the jet transverse momentum, covering the range from 100 GeV to 3.5 TeV, and the absolute jet rapidity up to |y|<3. In addition, the double-differential dijet production cross-sections are presented as a function of the dijet mass, covering the dijet mass from 300 GeV to 9 TeV and the half absolute rapidity separation between the two leading jets, y^*, up to $y^* < 3$. Figure 7 shows the individual components of the systematic uncertainties added in quadrature for the inclusive jet cross-section measurements in representative phase-space regions. The dominant systematic uncertainty arises from the jet energy scale.

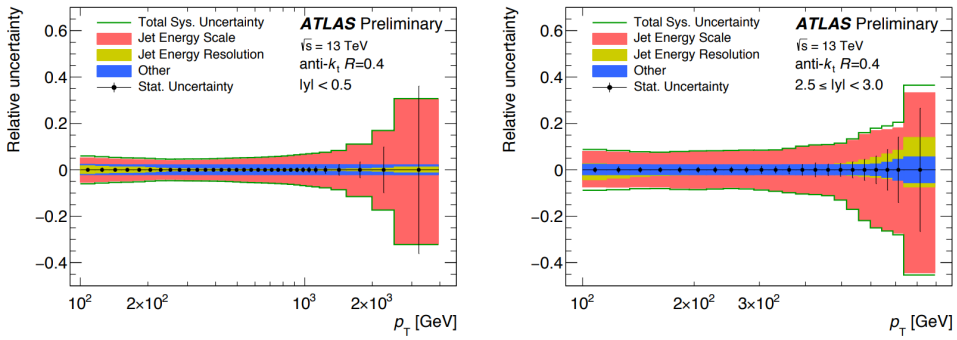

Figure 7. Relative systematic uncertainty for the inclusive jet cross-section as a function of the jet p_T for $|y| < 0.5$ (left) and $2.5 < |y| < 3$ (right). The individual uncertainties are shown in different colors: the jet energy scale, jet energy resolution and the other uncertainties (jet cleaning, luminosity and unfolding bias). The total systematic uncertainty, calculated by adding the individual uncertainties in quadrature, is shown as a green line. The statistical uncertainty is shown as vertical black bars [14].

NLO and NNLO pQCD calculations for the inclusive jet measurement, corrected for non-perturbative and electroweak effects, are compared to the measured cross-sections in figure 8. Similarly to the study at 8 TeV, a quantitative comparison of the measurements to fixed-order NLO QCD calculations shows overall fair agreement when considering jet cross-sections in individual jet rapidity bins independently. In the inclusive jet measurement, a strong tension (with p-values $\ll 10^{-3}$) between data and theory is observed when considering data points from all jet transverse momentum and rapidity regions. No significant deviations between the inclusive jet cross-sections and the fixed-order NNLO QCD calculations corrected for non-perturbative and electroweak effects are observed when using p_T^{jet} as QCD scale.

4 Transverse energy-energy correlations and the extraction of α_s

TEEC and ATEEC in multi-jet events have been measured using the ATLAS 8 TeV data set [15]. The data, binned in six intervals of the sum of transverse momenta of the two leading jets, $H_{T2} = p_{T1} + p_{T2}$, are corrected for detector effects and compared to the predictions of pQCD, corrected for hadronisation and multi-parton interaction effects. The results show that the data are compatible with the theoretical predictions, within the uncertainties.

The data are used to determine the strong coupling constant α_s and its evolution with the interaction scale $Q = (p_{T1} + p_{T2})/2$ by means of a χ^2 fit to the theoretical predictions for both TEEC and ATEEC in each energy bin. Additionally, global fits to the TEEC and ATEEC data are performed, as it is shown in figure 9, leading to

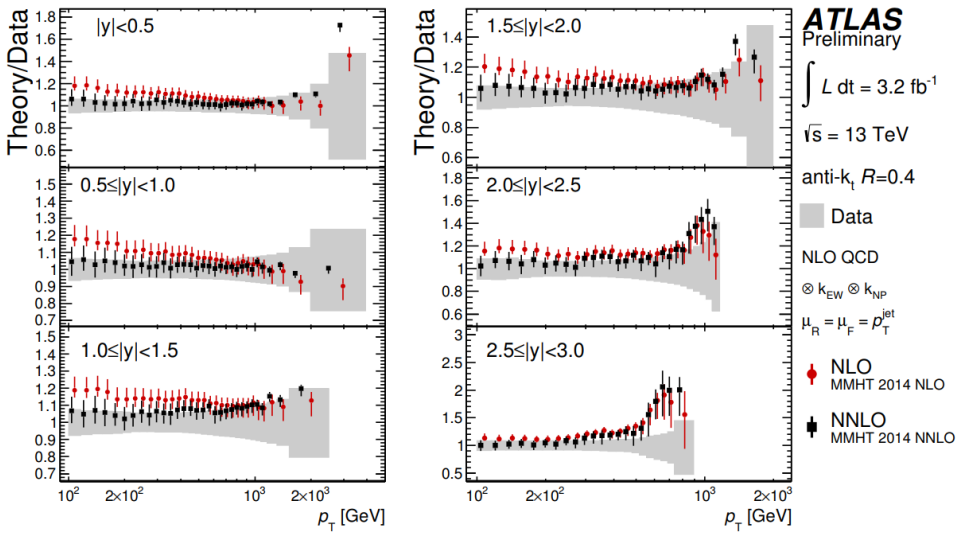

Figure 8. Ratios of the NLO and NNLO pQCD predictions to the measured inclusive jet cross-sections are shown as a function of the jet p_T in six |y| bins for anti-kt jets with R = 0.4 [14]. The NLO predictions are calculated using NLOJET++ with MMHT 2014 NLO PDF set. The NNLO predictions are provided by the authors of ref. [19, 20] using NNLOJET with p_T^{jet} as the QCD scale and the MMHT 2014 NNLO PDF set. Non-perturbative and electroweak corrections were applied to the predictions. The NLO and NNLO uncertainties are shown by the color lines. The grey band shows the uncertainty including both, systematic (JES, JER, unfolding, jet cleaning, luminosity) and statistical uncertainties.

$$\alpha_s(m_Z) = 0.1162 \pm 0.0011(exp.)^{+0.0076}_{-0.0061}(scale) \pm 0.0018(PDF) \pm 0.0003(NP),$$
$$\alpha_s(m_Z) = 0.1196 \pm 0.0013(exp.)^{+0.0061}_{-0.0013}(scale) \pm 0.0017(PDF) \pm 0.0004(NP),$$

respectively. Conservatively, the values obtained using the NNPDF 3.0 PDF set are chosen, as they provide the largest PDF uncertainty among the different PDF sets investigated. These two values are in good agreement with the determinations in previous experiments and with the current world average $s(m_Z) = 0.1181 \pm 0.0011$. The correlation coefficient between the two determinations is equal to 0.60. The present results are limited by the theoretical scale uncertainties, which amount to 6% of the value of $s(m_Z)$ in the case of the TEEC determination and to 4% in the case of the ATEEC. This uncertainty is expected to decrease as higher orders are calculated for the perturbative expansion.

5 Summary

High-precision measurements involving photons and jets on 8 TeV data are being complemented by the first results at 13 TeV. The ATLAS Collaboration has achieved a strong performance in jet and photon reconstruction and many of the results are now dominated by the uncertainties on the predictions and the PDFs. This highlights the importance of the NNLO predictions, which will reduce the renormalisation and factorisation scale uncertainty. Complex measurements of final states involving photons and jets explore regions of phase-space where the current theory struggles to match the data, providing valuable physics input to PDF and α_s fits, and to the description of various aspects of QCD radiation. Diphoton production processes are particularly sensitive to higher-order QCD phenomenology. For the future, the systematic exploration of more complex variables and final states,

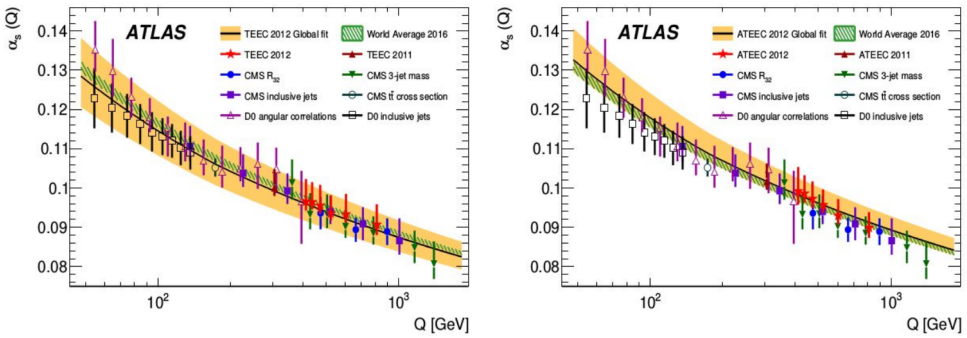

Figure 9. Comparison of the values of $\alpha_s(Q)$ obtained from fits to the TEEC (left) and the ATEEC (right) functions at the energy scales given by $< H_{T2} > /2$ (red star points) with the uncertainty band from the global fit (orange full band) and the 2016 world average (green hatched band) [15]. Determinations from other experiments are also shown as data points. The error bars, as well as the orange full band, include all experimental and theoretical sources of uncertainty. The strong coupling constant is assumed to run according to the two-loop solution of the RGE.

combining several beam energies, will be crucial for fine-tuning descriptions of the Standard Model, and providing precise background estimates for new physics searches.

References

[1] The ATLAS Collaboration, JINST *3* (2008)
[2] The ATLAS Collaboration, Physics Letters B *770* 473–493 (2017)
[3] Torbjörn Sjöstrand et al, Computer Physics Communications *Volume 178 Issue 11* 852-867 (2008)
[4] T. Gleisberg et al, JHEP 02 (2009) 007
[5] Stefano Catani et al, JHEP05(2002)028
[6] L.A. Harland-Lang et al, Eur. Phys. J. C 75 (2015) 204
[7] John M. Campbellet al, Phys. Rev. Lett. 118, 222001
[8] Schwartz, M.D. J. High Energ. Phys. (2016) 2016: 5
[9] The ATLAS Collaboration, PHYSICAL REVIEW D 95, 112005 (2017)
[10] T.Binoth et al, Eur. Phys. J. C 16, 311 (2000).
[11] C.Balaza et al, Phys. Lett. B 637, 235 (2006)
[12] S.Catani et al, Phys. Rev. Lett.108, 072001 (2012)
[13] The ATLAS Collaboration, J. High Energ. Phys. (2017) 2017: 20
[14] The ATLAS Collaboration, ATLAS-CONF-2017-048
[15] The ATLAS Collabotarion, arXiv:1707.02562 [hep-ex]
[16] The ATLAS Collaboration, Nucl.Phys. B918 (2017) 257-316
[17] C.F. Berger et al, Phys. Rev. D 78 (2008) 036003,
[18] The ATLAS Collaboration, ATLAS-CONF-2017-059
[19] J. Currie et al, Phys. Rev. Lett. 118 (2017)
[20] J. Currie et al, arXiv: 1704.00923 [hep-ex].